Chapter 5

Technologic Appliance and Performance Concerns in Wheelchair Racing – Helping Paralympic Athletes to Excel

Pedro Forte, Tiago M. Barbosa and Daniel A. Marinho

Additional information is available at the end of the chapter

http://dx.doi.org/10.5772/61806

Abstract

Numerical simulations have provided useful evidence in helping several sportsmen to excel in their field. This methodology aims to have a deeper understanding on the influence of equipment and sports techniques on sports performance. In wheelchair racing, technology was used without considering specific sport (some of the Paralympic sports used the same technology of their Olympic counterparts). It has induced unique changes in prosthetic and wheelchair devices. Eventually, technology has become an essential part of Paralympic sports, wheelchair-racing being one of the most popular events. Numerical simulations can help us gather evidence on the effects of drag force acting upon the athlete-chair system.

Different types of wheelchairs are designed for racing (track and road races), net, and invasion sports. One of the various strategies to enhance performance is to minimize the aerodynamic drag of the frame, tires, helmet, sports outfit, and body posture.

Numerical simulations can be used to predict the fluid dynamics.

The goal of this chapter is to review the state-of-the-art numerical simulations and suggest further studies in wheelchair racing. The chapter will include sections covering: (i) main determinants in wheelchair racing; (ii) the effect of aerodynamic force in in wheelchair racing performance; (iii) analytical models, experimental testing, and numerical simulations in wheelchair racing; and (iv) numerical simulations on equipment and techniques.

Keywords: CFD, Paralympic, Performance

1. Introduction

Wheelchair racing is a major event in Paralympics. This sport holds short (100m) to long distance (42km) races. The athletes are classified according to their condition into classes (T5i, i.e., i=1, 2, 3 and 4 with injuries at C5-6, C7-8, T1-7 and T8-S4 respectively) [1, 2]. In wheelchair racing, sports science has been expressed as a need in the modeling and computer simulations of racing wheelchairs and the racing itself [3, 4].

The first game for disabled persons, in pair with the Olympic Games, was held in Rome in 1960. Pioneer research on wheelchair racing happened in the 1980s which was based on high-speed films at laboratory or running track settings (5). In the 1980s, manufacturers estimated that more than 10,000 racing wheelchairs commercialized worldwide [6]. Being increasingly popular, the competitions between the contenders in these sports became tighter and research is eagerly needed to help Paralympic athletes to excel.

Nowadays, most world-ranked Paralympic athletes, including wheelchair racers, develop an evidence-based practice with the help of coaches and sports analysts. Every detail of a race is deeply examined to have a deeper insight of the determinant factors that might help them excel. The resistance acting on the wheelchair racer is one of the major concerns for practitioners. The resistance force having an opposite direction to the displacement must be minimized so that for a given amount of thrust, the subject can reach a higher acceleration and speed. Lately, a few research projects were reported in the literature under this topic. So, the aim of this chapter is to review the state-of-the-art numerical simulations in wheelchair racing and suggest further studies in this sport.

2. The wheelchair race

The stroke cycle in wheelchair racing is divided into two phases: the propulsion and the recovery phases (Figure 1). The propulsion phase is characterized by the tangential force applied to the handrim. In the beginning of the race, this phase should be its highest and longest contact time so that the mechanical impulse will also be high [7]. It represents 33% to 35% of the full stroke cycle. The remaining 65% to 67% of the stroke time is the recovery phase in elite wheelchair racers [8, 9, 7, 10]. In this phase, we have the time period that the hand does not contact the rims. The hand tends to follow different paths until being positioned in the rim again to a new propulsion phase [11-13]. However the recovering phase may change, the free chosen push frequency (the preferred stroke frequency adopted by each subject) ranged from 32 to 86 pushes/min at a 6.58 m/s in wheelchair racing.

The stroke cycle can also be divided into 5 moments: catch, drive, release, lift and stretch, and finally, acceleration. Catch is the hand contact moment on the handrim, it usually occurs nearly the 1 and 2 o'clock positions. Drive phase is the moment of the hand and wrist acceleration on the handrim and it usually occurs nearly the 2 and 5 o'clock. Release phase is the moment of the contact breaking of the hand with the handrim, closer to the 6 o'clock. Lift and stretch phase

http://dx.doi.org/10.5772/61806

is characterized by the elbow flexion and elevation in the sagittal plan. Acceleration moment is when the elbow extension is done before the handrim contact.

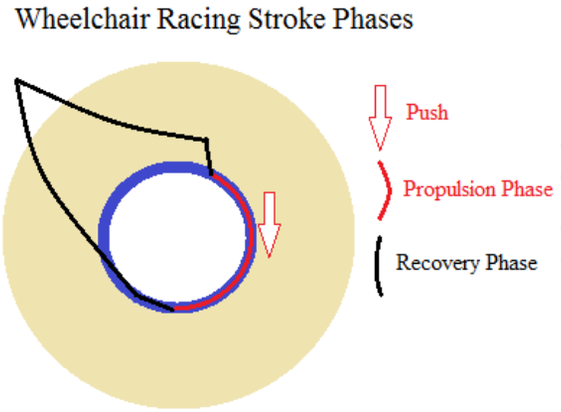

Figure 1. Stroke Cycle in Wheelchair Racing

During a race, the racers aim to reach the maximal speed as soon as possible and keep it for the remaining time (Figure 2). Figure 2 also depicts the intra-cycle speed (i.e. due to hand contact and recovery phase). This only proves that propulsive forces are higher than resistance forces (i.e. positive acceleration) at a given moment, and there are also moments that it will have higher intensity (i.e. negative acceleration).

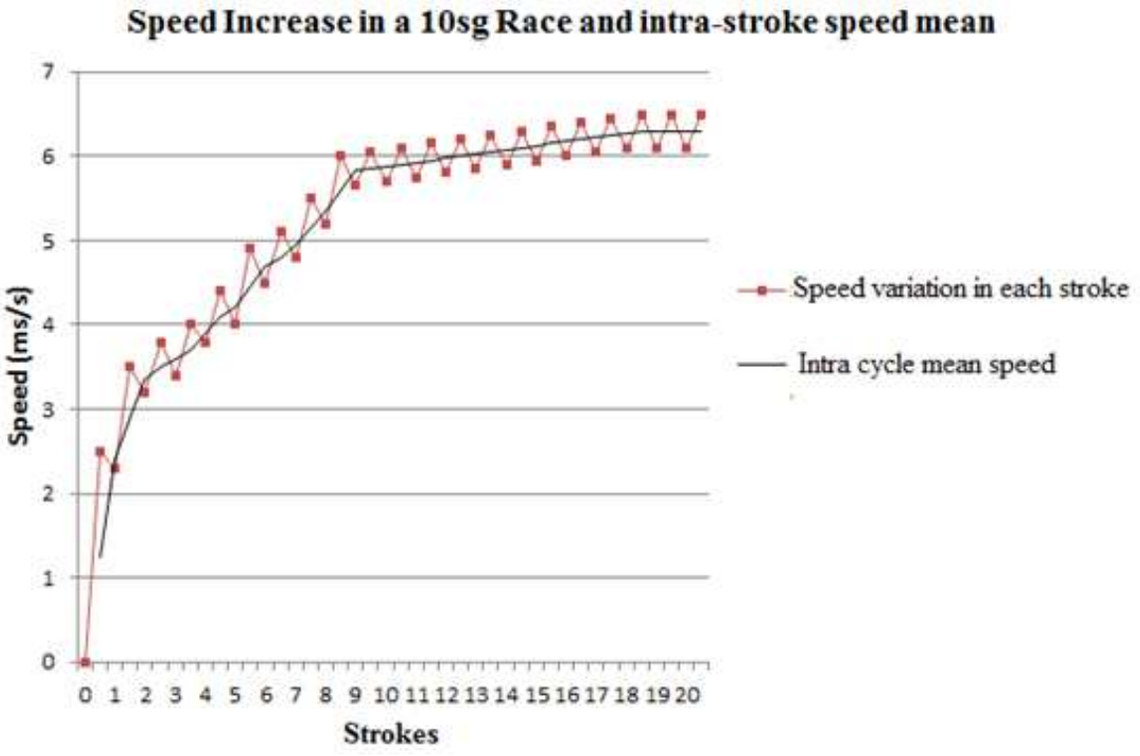

Figure 2. Theoretical Representation of the Speed over Time in 20 Stroke Cycles

Stroke kinematics is selected on a regular basis to report the stroke cycle. This includes the assessment of the average speed, stroke frequency, and stroke length.

The stroke frequency can be evaluated by measuring the number of cycles per minute and stroke speed given by the product of stroke length and stroke frequency. Stroke length is the difference between the contact distance of a stroke and the contact covered distance of the next stroke. Thus, stroke length can be explained as the covered distance with handrim contact in one stroke [14]. The average speed is calculated dividing the stroke length by the stroke frequency [14].

A higher stroke frequency combined with the hand linear velocity will lead to a greater energy cost, and probably will enhance cardiorespiratory stress affecting blood lactate and heart rate [15]. The increase of speed is related with blood lactate concentration and rise of heart rate. Despite this, the increase of the handrim diameter seems to reduce the blood lactate concentration at 20km/h, however it did not happen at 22km/h. [15].

An increased time of hand contact on the handrim without wrist acceleration will generate deceleration by friction resistance applied by the hand on the handrim. Therefore, to achieve a lower contact, it is recommended to produce a high speed soon after the start [16], which is possible to improve as demonstrated by sprinters in strength development [17]. The elbow motion seems to range from 60.9º to 5.2º in flexion to extension movement; and the maximum flexion velocity ranges from 515.4º/s and 572.8º/s, which is independent of the lightweight of the wheelchair. However, the propulsion arc reduces by 12º to 14º in the pumping-stroke technique that results from the shortest handrim contact possible, usually at the start of the race [18]. In the 1986 National Wheelchair Track and Field Championship in Illinois, in elite finalists both in paraplegic and quadraplegic wheelchair racers, the mean velocity-time ranged in each stroke from 5.1m/s to 5.5m/s and 3.7m/s to 4.27m/s respectively. The mean velocity in each stroke ranged 0.4m/s and 0.6m/s between the propulsion and recovery phase for the same subjects respectively. As the stroke frequency increases, velocity peak also enhances, despite the negative correlation between the velocity peak and the hand contact time with the handrim. The contact phase of the hand in handrim ranged from 13.58º to 15.6º for quadriplegics and paraplegics. The start acceleration phase at the rims starts at 48.54º and 71.1º. The break contact happens at 187.5º and 238.9º. The peak velocity for each stroke, occurs at 181.1º and 223.5º for quadriplegics and paraplegics respectively. These results were founded in a 10-second sprint with 20 to 25 propulsive cycles (strokes) for each subject [19].

The velocity peak seems to occur near the 10-second sprint in wheelchair track racers [7]. Wheelchair basketball players achieve 80% of the peak velocity in the first three strokes. On the other hand, wheelchair racers at the third stroke only achieve 55% of the peak velocity. The stroke frequency in short distances is greater than in long distances. In 10 seconds, sprints were obtained with 2 strokes per second [20]. However, in an 800m race, the stroke frequency ranged between 1.77 and 1.72 Hz [7].

http://dx.doi.org/10.5772/61806

3. Main determinants in wheelchair racing

The wheelchair racing athlete intends to reach the maximum acceleration as soon as possible. According to Newton's Second Law, the acceleration (a) is the ratio between force (f) and mass (m) (Equation 1).

$$a = \frac{F}{m} \tag{1}$$

In the wheelchair racing case, it is also possible to say that:

$$a = \frac{\left(F_{Prop} - F_{Resist}\right)}{m} \tag{2}$$

F_{Prop} and F_{Resist}, are the propulsive forces and the resistive ones respectively.

Positive acceleration is obtained by the applied propulsive forces on the wheels, overcoming the resistive ones (Figure 3). In wheelchair racing, the propulsive force is the push on the handrim, generating motion (i.e. the applied force by the ground in the wheel). The resistive forces are the rolling friction (Fr) and aerodynamic drag (Fd).

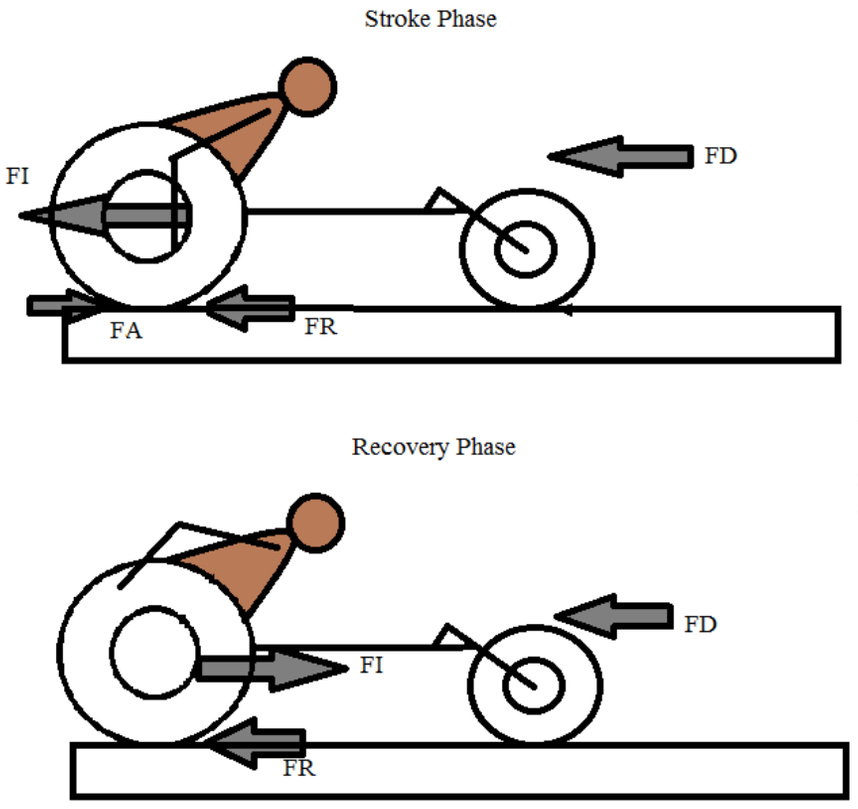

Figure 3. Free body diagram in wheelchair racing [21]; FI – Inertial force; FD – Drag force; FR – Rolling friction forces; FA – The applied force by the ground on the rear wheels.

Fuss [21] reported an analytical model to describe the performance based on these major determinants. The inertial force is the required force to change the body state and start the motion. The drag force is the air resistance to the wheelchair-athlete system. Rolling friction is the resistive force of the ground on the wheels' tires. Considering Newton's Third Law, the applied force by the ground on the rear wheel is the opposite one of the wheel in the ground derived by propulsion.

According to Fuss [21], the total energy expended by the athlete is taken by rolling friction and air drag. It is possible to say that the velocity is dependent on the kinetic energy of the system and its mass.

$$v = \sqrt{\frac{2\left(E_{in} - E_{loss}\right)}{m}} \tag{3}$$

In the equation, v is the velocity, E_{in} is the energy produced by the athlete and E_{loss} is the energy lost.

$$\mathrm{E_{kin}} = \mathrm{E_{input}} - \left(\mathrm{E_{drag}} + \mathrm{E_{friction}}\right) \tag{4}$$

The total kinetic energy is obtained from the sum of all mobile parts with a speed higher than zero. It is also considered that other movement oscillations do not contribute to the kinetic energy. Then:

$$E_{kin} = \frac{mv^2 + \sum_{i=1}^{3} I_i \omega_i}{2} \tag{5}$$

In Equation 5, Ii is the moment of inertia and ωi is the angular velocity of wheel i.

When the inertia force (FI) gets combined with distance, the kinetic energy (Ekin) can be formulated as:

$$E_{kin} = \int_{x1}^{x2} F_I d_x \tag{6}$$

Equations 7 and 8 consider that velocity comes from the work of the rear wheel (ωri) and acceleration is the angular velocity of the rear wheel (a = αri), then solving it for FI, we obtain:

$$F_I = a\left(m + \sum_{i=1}^{3} \frac{I_i}{r_i^2}\right) \tag{7}$$

http://dx.doi.org/10.5772/61806

In this formula, m is the mass of wheelchair-athlete system and I is obtained from the relation between the one wheel mass and the wheel radius gyration squared. The mass of one wheel multiplied by its radius of gyration squared when accelerated, an equivalent mass results in FI:

$$M = m + \sum_{i=1}^{3} \frac{I_i}{r_i^2} \tag{8}$$

The propulsion cycle is given by the stroke and recovery phases, the equilibrium forces in the stroke one are given by:

$$F_A + F_I + F_D + F_R = 0 \tag{9}$$

$$F_A + M_a + C_{Dv^2} + mg\mu_R + mgk_{fv^2} = 0 \tag{10}$$

C_D is the drag coefficient, v is the instantaneous velocity (considering distance and time at a given moment) and the acceleration (d^2x/ dt^2). The C_D cluster is obtained from $0.5\varrho cDA$, being the product of air density (ϱ) with the drag coefficient of the air (C_D) and the frontal surface area (A). Considering that wheelchairs are in straight line and according to Equation 14, 12 and 13, FR is given by:

$$F_R = \mu_R mg + k_f mgv^2 \tag{11}$$

Where μ_R is the rolling friction coefficient, m is the mass, g the gravitational acceleration and k_f the coefficient of speed.

$$F_A + M_a + c_1 v^2 + c_2 = 0 \tag{12}$$

C_1 is given by,

$$c_1 = C_D + mgk_f \tag{13}$$

And C2,

$$c_2 = mg\mu_R \tag{14}$$

Thereby, in a wheelchair-athlete system, the responsible variables for the energy losses are FD and FR and both forces are equal to zero in a loss-free environment.

4. Propulsion

In the propulsion phase, Fuss [21] described four forces as the main ones. The ground applied one at the rear wheel, aerodynamic drag force and the rolling friction one. When the mass gets accelerated, it produces an inertial force (FI). The kinetic energy derived from FI, is stored on the wheels, it depends of the moment of inertia and the angular speed of the wheels creating the system motion. The four forces in equilibrium are described as,

$$F_A + F_I + F_D + F_R = 0 \tag{15}$$

F_A is the force applied to the ground on the wheels derived from the tangential force applied on the handrim (F_I). For movement occurring, F_A must be higher than F_I, F_D and F_R.

Several investigations have been made to better understand the physiological factors and demands that may affect the wheelchair propulsion. Others, for instance, [10] presented the motion of the racing wheelchair derived by the sum of all external forces by:

$$F\left(R/r_{pr}\right) = My + Iv/R + I_f v/r + Fa + M_B/r_{ax} + M_b/r_{axf} + F_R + F_r + W\sin 0\left(x\right) \tag{16}$$

Where, "R/r_{pr}" represents the gear ratio of the handring to the wheel. F - The tangential force in the handrings; R and r_{pr} - The radius of the rear wheels and handrings; M - The mass of the system athlete-wheelchair; v - The velocity of the athlete-wheelchair system, given by: $v = x = dx/dt$; I and I_f - The inertia of the rear wheels and the wheels inertia; r - The radius of the front wheels; Fa - The air resistance of the athlete-wheelchair system; M_B - The rear hubs bearing resistance; M_b - The front hubs bearing resistance; r_{ax} and r_{axf} - The radius of the rear and front axles respectively; F_R and Fr- The rolling resistance of the rear and front wheels respectively; W - The weight of the athlete-wheelchair system; Θ (x) - The inclination angle (i.e., changes in elevation); x - The covered distance;

5. Inertia

The sum of the kinetic energy to all mobile parts is given by Equation 5. It includes the energy of the three wheels and the translational energy. The kinetic energy is equal to the inertial force combined with distance (Equation 6). Thus, the inertial force (F_I) is given by:

$$F_I = aM \tag{17}$$

M represents the sum of the inertial moments.

The Inertial Force is the required force for a body state change. At the beginning of the wheelchair race, the inertial force is the required force for starting the wheelchair. Therefore, it is clear that the mass influences the inertial moment in the system and that the mass reduction

http://dx.doi.org/10.5772/61806

will lead to a sooner and/or higher speed. Fuss [21] reported that a reduction of 1kg in a wheelchair-athlete system will improve the winning time by 0.132sg.

6. Air drag and rolling resistance

In wheelchair racing, the air drag results from the air resistance in the surface area of the athlete-wheelchair system. In contrast, the rolling resistance results from the friction of the tyres on the ground. Aerodynamic resistance can be minimized by reducing the frontal area of the subject, intending to improve the winning time of a racing wheelchair. At speeds greater than 5m/s aerodynamic drag represents 90% of the resistive forces [22]. Between 5.32m/s and 6.83m/s, rolling resistance is greater than aerodynamic drag with a partial contribution of 65% to 75% and 25% to 35% respectively. At greater speeds, aerodynamic drag starts to represent a greater contribution of the resistive forces [23].

Air drag and rolling resistance can be acceded from Equation 18 for rolling resistance and Equation 19 for air drag:

$$F_R = \mu_g mg + k_f mgv^2 \tag{18}$$

$$F_D = 0.5\rho A_d v^2 C_D \tag{19}$$

In these two equations, F_R is the rolling friction, μ_g is the rolling friction coefficient, m is the mass of the athlete-wheelchair system, g is the gravity acceleration and k_f is the coefficient of the speed influence in rolling resistance force, ϱ is the air density, A_d is the frontal area, v^2 is the velocity, and C_D is the drag coefficient.

Lightweight clothes should be worn by wheelchair racers to reduce the aerodynamic drag [23]. A flexed upper trunk position also reduces the aerodynamic drag, as does reducing the rear wheel spokes to 24 [22]. In cycling, a flexed upper trunk position reduces the frontal area in 20% to 29% [24]. In wheelchair racing, the same position reduces the frontal area in 3% to 4% [25].

Mass would also influence the rolling friction; reducing the wheelchair-athlete system would also improve the speed, mainly in short distances. A 1kg reduction would improve 1-2.3% of the winning time in wheelchair racing [21].

7. Analytical models, experimental testing, and numerical simulations in wheelchair racing

7.1. Experimental testing: Coast-down technique

Aerodynamic and rolling resistance can be tested providing realistic opportunities that cannot be achieved in laboratory. The coast-down methods founded in literature are: (i) roll distance

applying the ramp methods; (ii) the timing gate method that measures the velocity decrease in different points between two marks (gates); and (iii) the velocity method that measures directly the speed in each time.

The roll distance applying the ramp method consists rolling, a wheelchair from a ramp to the field, measuring the covered distance by the wheelchair [26]. The timing gate method was developed as an alternative to the roll distance, produced in less time and space compared with the whole roll until the wheelchair stops. Two marks should be performed counting the time when the wheelchair passes between them [27]. In the velocity method, the racer reaches the maximum speed, stops the propulsion and the velocity is recorded in each instance [27, 21]. A dynamometer-based coast-down test was used for the wheel deceleration calculus [28]. For wheel deceleration in each trial, hub (Hubxyz) and handrim (Rimxyz) markers were placed. The wheel rotation on each time was assessed by the law of cosines:

$$\theta = \cos^{-1}\left(\frac{A \times B}{\|A\| \, \|B\|}\right) \tag{20}$$

A = Rimxyz(i) – Hubxyz(i); B = Rimxyz (i + 1) – Hubxyz (i + 1).

To avoid wheel size differences, the angular speed was converted to linear one. It has fitted a line to the linear velocity (v) data intending to determine the wheel deceleration (ad), the time to coast down from 2 m/s to 1 m/s is represented by "t" and the initial wheel velocity is represented by "$v_{0''}$.

$$v = a_d t + v_0 \tag{21}$$

The estimation for rolling resistance can be done based on Cooper's method [10]. Intending to simplify the method, aerodynamic drag, wheel and roller bearing resistances, as other external resistances were neglected. Thus, the rear wheel motion was described by:

$$T_w = \left(I_r \frac{R}{r} I_w\right) a_w + F_{RR} R \tag{22}$$

Where, "T_w" was the torque applied by the hand to the rear wheel; "I_r" and "I_w" were the moment of inertia of the roller and the rear wheel, respectively; "r" and "R", the roller and rear wheel radius, respectively; "a_w" and "F_{RR}" as the angular acceleration of the rear wheel and the rolling resistance force respectively.

Considering that the propulsive force was discontinued, "T_w" is equal to zero, and "a_w" represents the wheel angular deceleration. The equation is being used to describe the rear wheel rotation. The roller inertial moments (0.87 ± 0.15 kg-m^2) and wheels (0.12 ± 0.02 kg-m^2) were experimentally acceded resourcing the acceleration method by DiGiovine et al. [29].

http://dx.doi.org/10.5772/61806

Applying the "I_r" and "r" values into Equation 22, and rewriting "a_w" as the ratio between linear deceleration and radius (a_d/R), rolling resistance force is obtained from the wheel radius, inertia, and deceleration, calculated by:

$$F_{RR} = \frac{-a_d}{R^2}\left(I_w + 5.47R\right) \tag{23}$$

Coast-down distance (CDD) calculation was computed using the equation of motion, where acceleration is assumed to be constant and t is the time for coast-down technique ends, when the wheelchair stops:

$$CDD = \frac{1}{2}a_d t^2 + v_0 t \tag{24}$$

Another method exists in accelerating the wheelchair (e.g., from 2.5 to 12.8m/s). The rider stops the propulsive phases reaching the target speed counting the length and/or time until the wheelchair stops [30]. In this method both aerodynamic drag and rolling resistance are obtained. Figure 4 depicts a speed decay of wheelchair considering the velocity method, measuring the speed in each time.

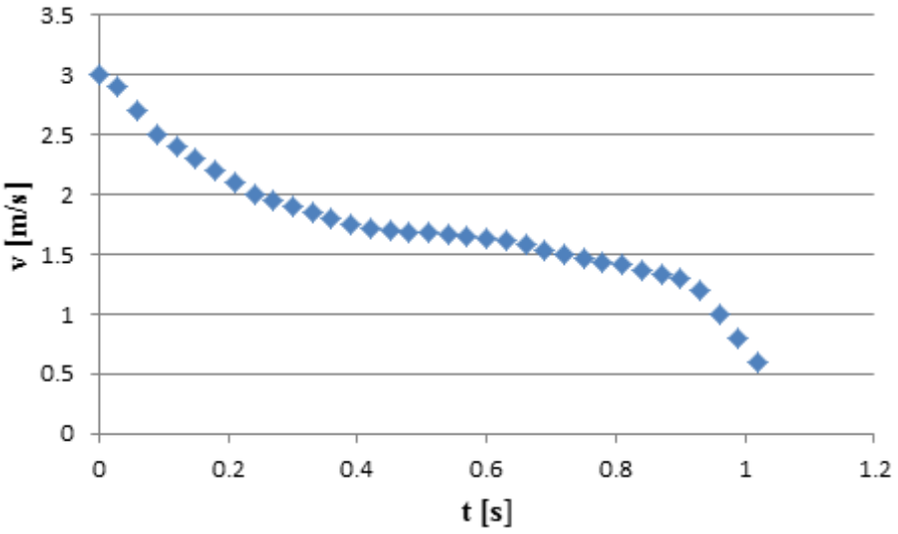

Figure 4. The Velocity Decay of a Manual Wheelchair over a Typical Trial

7.2. Wind tunnel testing

At least one paper can be found in the literature reporting the assessment of the aerodynamics in wind tunnel between two wheelchair models [31]. The drag forces were measured for speeds between 54.86km/h and 164.60km/h with intervals of 18.28km/h. However, air viscosity and

ground motion effect are not taken into account with this methodology. Aside from this, a better wind tunnel test should be performed intending to determine the best helmet and clothes to use in races [31]. The Drag was proportional with the speed in the two models A and B. Model A presented a strict nose, with fenders at the wheels and an exceeded front angle attack. The drag force was acceded in grams (gr) and ranged from 26(gr) to 360(gr) in both models, with and without pilot. With and without pilot, Model B presented a lower drag force for velocities lower than 91.44km/h. At higher speeds, Model A presented lower drag force with and without pilot.

From this experimental test, it is possible to confirm that specific wheelchairs should be made for specific racers, and a sprint race wheelchair should be different to a long race wheelchair.

7.3. Analytical method for drag assessment

For rolling friction and aerodynamic drag, Burton, Fuss & Subic [32] presented an analytical procedure to estimate rolling friction and aerodynamic drag. FR is non-linear when calculated from visco-elastic models, considering the deformation of the tyres, reduces in the ground higher speed in parabolic function. The equations for these two forces are expressed in Equations 18 and 19.

According to Fuss [21], based on vehicles' data [33], consider that the μ_g of a racing wheelchair is 0.01, K_f is $5x10^{-6}$ s^2m^{-2}, a mean speed of 10 m/s and a mass athlete-wheelchair system of 80kg the first and second term of the equation 22 is 7.85 and 0.35N.

In a partial contribution assessment of air drag, Barbosa et al. [23] assumed the air density of 1.2041 kg/m3 in the sea level at 20º C. The surface area was measured with the photogrammetric technique in the frontal plane and the drag coefficient was assumed to be 0.7. All estimations were completed in each speed moment between 0 m/s and 13m/s increasing in every 0.1m/s. considering the world speed record, the air drag represents 34.89%.

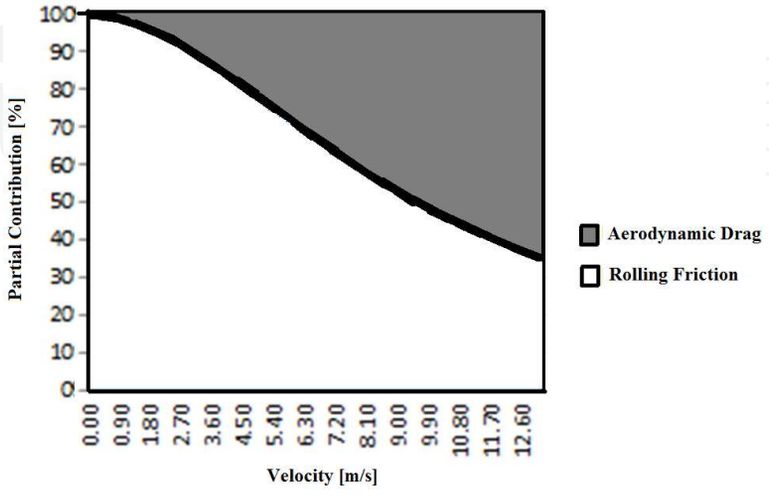

Figure 5. Partial Contribution of Aerodynamic Drag and Rolling Friction by Barbosa et al. [23].

http://dx.doi.org/10.5772/61806

7.4. Numerical simulations: Computer fluid dynamics

Computational Fluid Dynamics (CFD) has been used over the last 20 years. There are a lot of benefits on CFD and tools, such as FLUENT, CFX, STAR-CD and FiDAP, are all commercially available and used in industrial settings in the engineering community since the 1990s. Engineers and scientists started to use these simulations in competitive sports to reach a performance advantage, to improve sports equipment design and elite athletes' aerodynamics or hydrodynamic enhancements [34].

In sport sciences, the CFD presented concordance between numerical simulations and in vivo tests. For the simulation, a 3D body model scan is required and the images processing can be made with recourse to Anatomics Pro (Anatomics, Kannapolis, NC, USA) and FreeForm (Sensable Technologies, Woburn, MA, USA). The scan files are saved as IGES (*.igs) format, intending to be executable in Gambit/FLUENT (FLUENT Inc, Hanover, NH, USA). In Gambit/FLUENT, it is possible to generate the greed and to define the finite elements in 3D areas.

The numerical simulation consists discretization of Navier-Stokes equations by the finites volumes methods. These equations come from Newton's Second Law in fluid mechanics, assuming that the fluid stress is the sum of diffusion of its viscosity, resulting from an applied pressure term. The equation resolution determines the fluid speed in a determined point at space and time. CFD is based on an approximated finite volume. In this approximation, space is divided into small cells to form a mesh or greed, applying a solver algorithm for the equations of fluid volume motion resolution [35, 36].

The Reynolds-Averaged Navier-Stokes (RANS) comes from decomposing the instantaneous values into means and/or fluctuating components. Fluid flow behavior (Equation 25), Reynolds stresses (Equation 26), temperature (Equation 27) and mass transfer (Equation 28) can be solved in this methodology.

$$\frac{\partial_{\mathrm{Ui}}}{\partial_{\mathrm{xi}}} = 0 \tag{25}$$

$$\frac{\partial_{Ui}}{\partial_t} \pm U_j \frac{\partial_{Ui}}{\partial_{x_j}} = -\frac{1}{\rho}\frac{\partial P}{\partial x_j} + \frac{\partial}{\partial x_j}\left(2vS_{ij} - \overline{\mu_j'\mu_i'}\right) \tag{26}$$

$$\frac{\partial_{\theta i}}{\partial_t} \pm U_j \frac{\partial_{\theta}}{\partial_{x_j}} = \frac{1}{\rho_{cp}}\frac{\partial}{\partial x_j}\left(k\frac{\partial\theta}{\partial x_j} - \overline{\mu_j'\theta'}\right) \tag{27}$$

$$\frac{\partial_C}{\partial_t} \pm U_j \frac{\partial_C}{\partial_{x_j}} = \frac{\partial}{\partial x_j}\left(D\frac{\partial C}{\partial x_j} - \overline{\mu_j'c'}\right) \tag{28}$$

The μ_i and x_i are the instantaneous velocity and the position, p the instantaneous pressure, t is the time, ϱ the fluid density, v is the molecular kinematic viscosity, c_p heat capacity, k is the thermal conductivity and S_{ij} the strain-rate tensor, c is the instantaneous concentration, and D is the molecular diffusion coefficient.

The Reynolds stresses component ($\overline{\mu_j'\mu_i'}$), describes the turbulence of the mean flow being the exchange of momentum by the change of the fluid parcels. In a laminar flow, the molecules are the responsible for momentum exchange (molecular viscosity). However, in a turbulent flow (turbulent viscosity) the parcels of flow are the ones that exchange the momentum. To finish this calculus, it is also necessary to use a turbulence model to represent flow scales. The first order Boussinessq eddy-viscosity hypothesis to model the Reynolds stress in function of velocity and time is used. However, it is also a necessary model for the linear or non-linear eddy-viscosity distinction. The Reynolds stress is given by:

$$\overline{\mu_j'\mu_i'} = 2v_t S_{ij} - \frac{2}{3}k\delta_{ij} \tag{29}$$

v_t is the turbulent viscosity and the mean strain rate S_{ij} is given by,

$$S_{ij} = \frac{1}{2}\left(\frac{\partial U_i}{\partial_{xj}} + \frac{\partial j}{\partial_{xi}}\right) \tag{30}$$

The turbulent kinetic energy (k) is given by,

$$k = \frac{1}{2}\overline{\mu_i'\mu_i'} \tag{31}$$

And the Kronecker delta (δ_{ij}),

$$\delta_{ij} = \begin{cases} 1; if\ i = j \\ 0; if\ i \neq j \end{cases} \tag{32}$$

Assuming the gradient diffusion (Gradient-diffusion Assumption) for heat and mass fluxes, as function of the temperature gradients in the mean flow, the turbulence hot flow is given by,

$$-\overline{\mu_j'\theta'} = D_{\theta t}\frac{\partial \vartheta}{\partial_{xi}} \tag{33}$$

$D_{\theta t}$ is the turbulent heat diffusivity (turbulent Prandtl number), and $\frac{\partial \vartheta}{\delta_{xi}}$ is the temperature gradient in the mean flow. The turbulent Prandtl number is obtained by,

http://dx.doi.org/10.5772/61806

$$Pr_t = \frac{v_t}{D_{\theta,t}} \tag{34}$$

And the turbulent mass flow $-\overline{\mu_j' c'}$ is given by,

$$-\overline{\mu_j' c'} = D_{c,t} \frac{\partial C}{\partial x_i} \tag{35}$$

$D_{c,t}$ is the turbulent mass diffusivity (turbulent Schmidt number) and $\frac{\partial C}{\partial x_i}$ the concentrated gradient in the mean flow. The turbulent Schmidt number is calculated from Equation 36,

$$Sc_t = \frac{v_t}{D_{\theta,t}} \tag{36}$$

Once RANS needed a turbulence model, less expensive equations are created with additional variables, transforming in meanings of the instantaneous equations calculations. This results from removing several small equations and adding other unknown variables, determined by the turbulence models. Standard K – ε turbulence model used by [37] in a computational simulation on a counter-clock cyclist helmet, however, it is only valid in a completely turbulent fluid. The same mode is assumed for wheelchair racing. In FLUENT, the turbulence models available are: (i) Standard K – psilon; (ii) Standard K – ε; (iii) Spalart – Allmoras; (iv) Reynolds Stress (RSM) [38].

In this model (Standard K – ε) the Bussinesq hypothesis is given by,

$$-\rho \overline{\mu_i' \mu_j'} = 2\mu_t S_{ij} - \frac{2}{3}\rho k \delta_{ij} \tag{37}$$

Where the turbulent viscosity,

$$\mu_t = \rho C_\mu \frac{k^2}{\varepsilon} \tag{38}$$

The mean tension rate is given by Equation 30. The kinetic energy of turbulent fluctuation and the dissipation of the kinetic energy (m^2/s^2) are given by Equations 31 and 40 respectively.

$$k = \frac{1}{2}\overline{\mu_i' \mu_i'} = \frac{1}{2}\overline{\mu'^2} + \overline{v'^2} + \overline{w'^2} \tag{39}$$

k, is the energy measuring associated with the turbulent fluctuations in the flow.

$$\varepsilon = v\overline{\frac{\partial \mu'_i \partial \mu'_i}{\partial x_j \partial x_j}} \tag{40}$$

ε, is caused by the work of the smallest eddies against the viscous stresses in the flow.

Then the determination of k (Equation 41) and ε (Equation 42) by their transport equations are,

$$\rho\frac{\partial k}{\partial t} + \rho\frac{\partial}{\partial x_i}\left(k\mu_i\right) = \frac{\partial}{\partial x_j}\left(\left(\mu + \frac{\mu_t}{\sigma_k}\right)\frac{\partial k}{\partial x_j}\right) + G_k + G_b - \rho\varepsilon \tag{41}$$

$$\rho\frac{\partial \varepsilon}{\partial t} + \rho\frac{\partial}{\partial x_i}\left(\epsilon\mu_i\right) = \frac{\partial}{\partial x_j}\left(\left(\mu + \frac{\mu_t}{\sigma_\varepsilon}\right)\frac{\partial \varepsilon}{\partial x_j}\right) + C_{1\varepsilon}\frac{\varepsilon}{k}\left(G_k + C_{3\varepsilon}G_b\right) - \rho C_{2\varepsilon}\frac{\varepsilon^2}{k} \tag{42}$$

Where, $\rho\frac{\partial \varepsilon}{\partial t}$ and $\rho\frac{\partial k}{\partial t}$ are the variation of the local in time, $\rho\frac{\partial}{\partial x_i}(k\mu_i)$ and $\rho\frac{\partial}{\partial x_i}(\mu_i)$ the adjective term, $\frac{\partial}{\partial x_j}\left(\left(\mu + \frac{\mu_t}{\sigma_k}\right)\frac{\partial k}{\partial x_j}\right)$ and $\frac{\partial}{\partial x_j}\left(\left(\mu + \frac{\mu_t}{\sigma_\varepsilon}\right)\frac{\partial \varepsilon}{\partial x_j}\right)$ are the diffusion, G_k is the generation of k by the gradients mean velocity, G_b the generation of k due the fluctuation and ϱε the dissipation of k. σk and σε are the turbulent Prandtl numbers for k and ε respectively. And the constants $C_{1\varepsilon}$, $C_{2\varepsilon}$, C_μ, σ_k e σ_ε were experimentally determined, $C_{1\varepsilon} = 1.44$; $C_{2\varepsilon} = 1.92$; $C_\mu = 0.09$; $\sigma_k = 1.0$; $\sigma_\varepsilon = 1.3$.

The Gambit software allows the building of a representative graphic model of the volume subdivided in sub-volumes, trying to make the process as realistic as possible. This software also allows defining the frontiers. In solid frontiers and close to them, the FLUENT software computes the Reynolds tension and ε. It applies solid specific frontiers conditions for Reynolds tension using balance hypotheses, without considering the convection and diffusion of tension transport (Equation 25). In a local coordinate system, T is tangential coordinate, η the normal and λ the binomial one. The Reynolds tension in the adjacent cells to the frontier, are calculated by the equation:

$$\frac{\overline{\mu'^2_{\text{ﻫ}}}}{k} = 1.098,\ \frac{\overline{\mu'^2_{\eta}}}{k} = 0.247,\ \frac{\overline{\mu'^2}}{k} = 0.655,\ \frac{\overline{\mu'_t\mu'_\eta}}{k} = 0.255 \tag{43}$$

FLUENT solves the transport equation (41) for k obtaining. For calculus convenience, the equation is globally solved, albeit the calculus of the k values is only necessary near the frontier. In the rest of the domain, the k is calculated by the equation (26).

The mesh can be constructed by quadrangular elements, with a space size of 0.1mm. The resulting data from the computational simulation of the determined flow regime and the visualization of the pressure profiles and speed are obtained by FLUENT. The data processing allows calculating the drag coefficient in the diverse forms [39].

http://dx.doi.org/10.5772/61806

7.5. Numerical simulations on wheelchair racing

CFD methodology starts being used for equipment tests. In wheeler riders' helmets, CFD has shown that airflow velocities could be improved with grooves in polymer foam liner and also improving the sweat evaporation. A top helmet hole would improve the velocity in that point, however velocities at the back became lower [40].

The ideal posture and some changes in the wheelchair could be possible to define the three first places. The tests revealed that the most drag negative influence in performance came from the athlete and not from the wheelchair. With a subtle modification in the sitting position, it could save 10% of the aerodynamic drag. No results were presented by the authors relatively to the wind tunnel test [41].

CFD methodology must be applied in different fabrics, helmets, and wheelchairs. The frame design, as the tube sizes must influence the fluid flow behavior. Also, different positions should be considered to be analyzed the flexed head in the start of the race or the look forward position. In each stroke phase, the different fluid flows should also be analyzed intending to reach the ideal motion in the stroke phase and recovery one, as the effect of the wheelchair designs and materials in the fluid flow [23].

Thus, fluid dynamics analysis should be performed intending to evaluate possible different designs of the wheelchairs and fulfill the lack of literature in this area. There is a need of results presentation such as drag and drag coefficient in different positions, helmets, and cloths at different speeds.

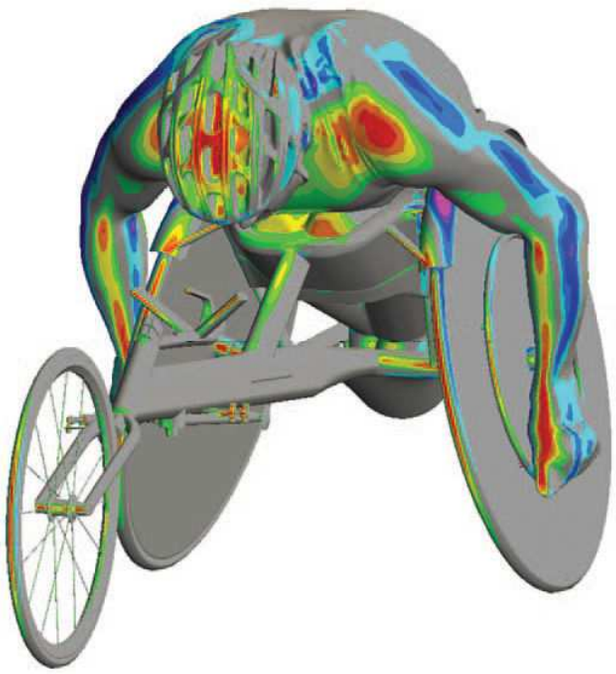

Figure 6. CFD Methodology of a Scanned Model in TotalSim (http://www.totalsimulation.co.uk/wp/cfd-image-gallery/)

8. Summary and conclusions

The sports science of wheelchair racing lacks research. However, there is some information that could positively contribute to increase performance in athletes. Managing the mathematical models based on Physics laws, coaches could identify the mechanic performance obstacles and try to minimize them.

The drag reduction by the rolling and air resistance access also contributed to increase the performance in athletes. Better propulsion could be obtained by reducing the total drag combined with a mass reduction and other possible aerodynamic positions. The purpose of computational simulations and/or computer fluid dynamics is the time improvement achieved by reducing the aerodynamic drag. No data was found about CFD tests in wheelchair racing.

The stroke technique should also be focused, despite the lack of indications about the number of hours off training after an injury occurrence. It is defined that the high angular velocities near the shoulder and the elbow generated by the strokes induce an overuse stress increasing the risk for joint injuries. There are also some indications about the contact zones, force applying, and contact break at the rear wheels.

Physiological variables should also be studied in wheelchair racing athletes, an area that lacks information in this sport. Thus, a precise control of the total drag and the efficiency of the stroke technique, which is related to high levels of strength derived by the strength and physical condition training, will positively contribute for a better performance.

Author details

Pedro Forte[1,2], Tiago M. Barbosa[2,3] and Daniel A. Marinho[1,2*]

*Address all correspondence to: dmarinho@ubi.pt

1 University of Beira Interior, Department of Sport Sciences, Covilhã, Portugal

2 Research Centre in Sports, Health and Human Development, Covilhã, Portugal

3 National Institute of Education. Nanyang Technological University, Singapore

References

[1] IWAS (2008) IWAS Athletics, worldwide ranking. http://athletics.iwasf.com/. Accessed 14 Aug 2009

[2] IPC International Paralympic Committee (2007) IPC athletics classification manual for physical impairments 2008–2010. http://www.paralympic.org/release/Summ-

er_Sports/Athletics/News/2007_12_07_ClassificationManual.pdf. Accessed 14 Aug 2009.

[3] Depauw, K. P. (1986). Research on sport for athletes with disabilities. Adap Phys Activ Q, 3(4): 292-299.

[4] Depauw, K. P. (1988). Sports for individuals with disabilities: Research opportunities. Adap Phys Activ Q, 5: 80-89.

[5] Cooper, R. A. (1990c). Wheelchair racing sports science: a review. Journal of rehabilitation research and development, 27(3), 295-312.

[6] Lakomy, H. K. A., Cambell, I. & Williams, C. (1987). Treadmill performance and selected physiological characteristics of wheelchair athletes. Br J Sports Med, 21(3), 130-133.

[7] Ridgway, M., Pope, C., Wilkerson, J. (1988). A kinematic analysis of 800-meter wheelchair racing techniques. Adapt Phys Act Q 5(2): 96-107.

[8] Bymes, D.P. (1983). APlm and EMG drive phase analysis of the competitive wheelchair stroke. Unpublished master's thesis, University of Alberta.

[9] Cooper, R. A. (1990b) An exploratory study of racing wheelchair propulsion dynamics. Adapt Phys Act Q, 7(1): 74-85.

[10] Sanderson, D. J., Sommer, H. J. (1985). Kinematic features of wheelchair propulsion. J Biomech 18(6): 423-429.

[11] Cooper, R. A. (1990). A systems approach to the modeling of racing wheelchair propulsion. J Rehabil Res Dev, 27(2): 151-62.

[12] Davis, R., Ferrara, M., & Byrnes, D. (1988). The competitive wheelchair stroke. NSCA Journal, 10(3), 4-10.

[13] Higgs, C. (1985). Propulsion of racing wheelchairs. In C. Sherrill (Ed.), Sport and disabled athletes (pp. 165-172). Champaign, IL: Human Kinetics

[14] Chow, J. W., Chae, W. (2007). Kinematic analysis of the 100 m wheelchair race. J Biomech, 40: 2564–2568.

[15] Costa, G. B., Rubio, M. P., Belloch, S. L., & Soriano, P. P. (2009). Case study: effect of handrim diameter on performance in a paralympic wheelchair athlete.Adapted physical activity quarterly, 26(4), 352-363.

[16] O'Connor, T., Robertson, R. N., Cooper, R. A. (1998). Three-dimensional kinematic analysis and physiologic assessment of racing wheelchair propulsion. Adapt Phys Activ Q, 15: 1–14.

[17] Keogh, J. W. L. (2011). Paralympic sport: an emerging area for research and consultancy in sports biomechanics. Sports Biomech, 10: 249–268.

[18] Rudins, A., Laskowski, E. R., Growney, E. S., Cahalan, T. D., & An, K. N. (1997). Kinematics of the elbow during wheelchair propulsion: a comparison of two wheelchairs and two stroking techniques. Archives of physical medicine and rehabilitation, 78(11), 1204-1210.

[19] Gehlsen, G. M., Davis, R. W., & Bahamonde, R. (1990). Intermittent velocity and wheelchair performance characteristics. Adapted Physical Activity Quarterly, 7(3), 219-230.

[20] Coutts, K. D. (1990). Kinematics of sport wheelchair propulsion. Journal of rehabilitation research and development, 27(1), 21-26.

[21] Fuss, F. K. (2009). Influence of mass on the speed of wheelchair racing. Sports Engineering, 12(1): 41-53.

[22] LaMere, T.J., & Labanowich, S. (1984). The history of sports wheelchairs: Part III, The racing wheelchair 1976-1983. Sports 'n Spokes, 10 (1), 12-16.

[23] Barbosa, T. M., Forte, P., Morais, J. E., Coelho, E. (2014). Partial contribution of rolling friction and drag force to total resistance of an elite wheelchair athlete. 1st International Conference in Sports Sciences & Technology. ICSST, Advanced Materials for Sport Technology, 749-753.

[24] Burke, E. (Ed.). (1986). Science of cycling. Champaign, IL: Human Kinetics Publishers.

[25] Hedrick, B., Wang, Y. T., Moeinzadeh, M., & Adrian, M. (1990). Aerodynamic positioning and performance in wheelchair racing. Adapted Physical Activity Quarterly, 7(1).

[26] FIFA. (2001). Quality Concept for Football Turf. Available: http://www.fifa.com/mm/document/afdeveloping/pitchequip/fqc_football_turf_folder_342.pdf.

[27] Kolitzus, H. J. (2003). Ball Roll Behavior: The Functional Relationship of the Ball Roll Distance and the Timing Gate Method; How to Calculate the Ball Roll Distance from Timing Gate Measurements. ISSS - International Association for Sports Surface Sciences, Eschenz / Switzerland, Available: http://www.isss-sportsurfacescience.org/downloads/documents/ZPKPAJJUWY_Ball_Roll_BehaviorKS.pdf.

[28] Kwarciak, A. M., Yarossi, M., Ramanujam, A., Dyson-Hudson, T. A., & Sisto, S. A. (2009). Evaluation of wheelchair tire rolling resistance using dynamometer-based coast-down tests. J Rehabil Res Dev, 46(7), 931-38.

[29] DiGiovine CP, Cooper RA, Boninger ML. Dynamic calibration of a wheelchair dynamometer. J Rehabil Res Dev. 2001;38(1):41–55.

[30] Candau, R. B., Grappe, F., Menard, M., Barbier, B., Millet, G.Hoffman, M. D. 1999. Simplified deceleration method for assessment of resistive forces in cycling. Medicine and Science in Sports and Exercise, 31: 1441–1447.

[31] MacLeish, M. S., Cooper, R. A., Harralson, J., & Ster, J. F. (1993). Design of a composite monocoque frame racing wheelchair. Journal of rehabilitation research and development, 30, 233-233.

[32] Burton, M., Fuss, F. K., & Subic, A. (2010). Sports wheelchair technologies. Sports Technology, 3(3), 154-167.

[33] Petrushov, V. A. (1998). Improvement in vehicle aerodynamic drag and rolling resistance determination from coast-down tests. Proceedings of the Institution of Mechanical Engineers, Part D: Journal of Automobile Engineering, 212(5), 369-380.

[34] Hanna, R. K. (2012). CFD in Sport-a Retrospective; 1992-2012. Procedia Engineering, 34, 622-627.

[35] Marinho, D. A., Barbosa, T. M., Mantha, V., Rouboa, A. I., & Silva, A. J. (2012). Modelling propelling force in swimming using numerical simulations. In: Juarez LH (Ed). Fluid Dynamics, Computational Modeling and Applications. Pp. 439-448. InTech. Rijeka.

[36] Marinho, D.A., Silva, A.J., Reis, V.M., Barbosa, T. M., Vilas-Boas, J.P., Alves, F.B., Machado, L., Rouboa, A. (2011) Three-dimensional CFD analysis of the hand and forearm in swimming. Journal of Applied Biomechanics. ISSN 1065-8483. 27:1, p. 74-80.

[37] Caboz, E. B. (2010). Simulação computacional do escoamento em torno de um capacete de ciclista usado nas provas de contra-relógio. Dissertação de mestrado. Faculdade de Engenharia da Universidade do Porto.

[38] White, F. (1999). Mecanica dos Fluidos, Ed. McGraw -Hill, 4ª edicao. ISBN : 85-86804-24-X.

[39] Carvalho, F. (2008). A aplicação da dinâmica computacional de fluidos no estudo do arrasto hidrodinâmico na natação. Dissertação de Mestrado em Educação Fisica e Desporto. Universidade de Trás os Montes. Vila Real.

[40] Pinnoji, P. K., & Mahajan, P. (2006, September). Impact analysis of helmets for improved ventilation with deformable head model. In Proceeding of IRCOBI conference, Madrid (pp. 159-70).

[41] Rushby-Smith, T., & Douglas, L. (2012). Paralympic Technology. Ingenia, 51, p.33.

IntechOpen